frontiers in
NEUROENERGETICS

ORIGINAL RESEARCH ARTICLE
published: 06 June 2011
doi: 10.3389/fnene.2011.00003

Compartmentalized cerebral metabolism of [1,6-^{13}C]glucose determined by *in vivo* ^{13}C NMR spectroscopy at 14.1 T

João M. N. Duarte[1,2]*, Bernard Lanz[1] and Rolf Gruetter[1,3,4]

[1] *Center for Biomedical Imaging, Ecole Polytechnique Fédérale de Lausanne, Lausanne, Switzerland*
[2] *Faculty of Biology and Medicine, University of Lausanne, Lausanne, Switzerland*
[3] *Department of Radiology, University of Lausanne, Lausanne, Switzerland*
[4] *Department of Radiology, University of Geneva, Geneva, Switzerland*

Edited by:
Sebastián Cerdán, Instituto de Investigaciones Biomédicas Alberto Sols, Spain

Reviewed by:
Sebastián Cerdán, Instituto de Investigaciones Biomédicas Alberto Sols, Spain
Kevin L. Behar, Yale University, School of Medicine, USA
Tiago B. Rodrigues, Cancer Research UK (Cambridge Research Institute) and University of Cambridge, UK

****Correspondence:***
João M. N. Duarte, Ecole Polytechnique Fédérale de Lausanne, SB IPMC LIFMET (Bâtiment CH), Station 6, CH-1015 Lausanne, Switzerland.
e-mail: joao.duarte@epfl.ch

Cerebral metabolism is compartmentalized between neurons and glia. Although glial glycolysis is thought to largely sustain the energetic requirements of neurotransmission while oxidative metabolism takes place mainly in neurons, this hypothesis is matter of debate. The compartmentalization of cerebral metabolic fluxes can be determined by ^{13}C nuclear magnetic resonance (NMR) spectroscopy upon infusion of ^{13}C-enriched compounds, especially glucose. Rats under light α-chloralose anesthesia were infused with [1,6-^{13}C]glucose and ^{13}C enrichment in the brain metabolites was measured by ^{13}C NMR spectroscopy with high sensitivity and spectral resolution at 14.1 T. This allowed determining ^{13}C enrichment curves of amino acid carbons with high reproducibility and to reliably estimate cerebral metabolic fluxes (mean error of 8%). We further found that TCA cycle intermediates are not required for flux determination in mathematical models of brain metabolism. Neuronal tricarboxylic acid cycle rate (V_{TCA}) and neurotransmission rate (V_{NT}) were 0.45 ± 0.01 and 0.11 ± 0.01 μmol/g/min, respectively. Glial V_{TCA} was found to be 38 ± 3% of total cerebral oxidative metabolism, accounting for more than half of neuronal oxidative metabolism. Furthermore, glial anaplerotic pyruvate carboxylation rate (V_{PC}) was 0.069 ± 0.004 μmol/g/min, i.e., 25 ± 1% of the glial TCA cycle rate. These results support a role of glial cells as active partners of neurons during synaptic transmission beyond glycolytic metabolism.

Keywords: glucose metabolism, neurotransmission, mathematical modeling, NMR spectroscopy, neurotransmitter metabolism

INTRODUCTION

Cerebral function depends on coordinated interaction of distinct cell types, namely neurons and glial cells, and relies on high metabolic activity that is supported by continuous and adequate supply of glucose and oxygen from the blood stream (Siesjo, 1978). Regulation of neuronal-glial cooperation at metabolic level involves the mechanism of deactivation of the major excitatory neurotransmitter, glutamate, through glial uptake and conversion to electrophysiologically inactive glutamine, which is then transported back to the neuron to replenish the neurotransmitter pool of glutamate (see revision by Zwingmann and Leibfritz, 2003). The maintenance of this exchange of glutamate and glutamine between neurons and glia requires energy provided by glucose oxidation in glycolysis and tricarboxylic acid (TCA) cycle (e.g., Sibson et al., 1998).

Although brain activity relies on blood glucose, it is not excluded the possibility of lactate exchange between metabolic compartments. In fact, a putative lactate shuttle is thought to exist from astrocytes to neurons (Magistretti et al., 1999). According to this hypothesis, most glucose is oxidized to lactate in astrocytes and the resulting adenosine-5′-triphosphate (ATP) suffices to maintain glutamate clearance from the synaptic cleft and conversion to glutamine. The produced lactate is transferred to neurons for oxidative degradation (Pellerin and Magistretti, 1994; Magistretti et al., 1999). Based on this hypothesis, glial metabolism has been thought to be mostly glycolytic (Sibson et al., 1998; Shulman et al., 2003), which is controversial (e.g., Dienel and Hertz, 2001; Gjedde and Marrett, 2001; Simpson et al., 2007; Mangia et al., 2009). Furthermore, astrocytic uptake of glutamate could also be fueled by ATP of mitochondrial origin (Dienel and Hertz, 2001) and, in fact, the glial TCA cycle was found to account for 30% of total TCA cycle activity in the conscious rat brain (Oz et al., 2004). A substantial fraction of mitochondrial oxidation in astrocytes occurs through pyruvate carboxylase and was suggested to increase with cerebral activity (Sibson et al., 1998; Choi et al., 2002; Oz et al., 2004).

The compartmentalization of these metabolic pathways and inter-compartmental interactions have been studied by non-invasive ^{13}C nuclear magnetic resonance (NMR). Dynamic

Abbreviations: ATP, Adenosine-5′-triphosphate; FE, fractional enrichment; NMR, nuclear magnetic resonance; PCA, perchloric acid; TCA, tricarboxylic acid.

in vivo ^{13}C NMR spectroscopy combined with the infusion of ^{13}C-enriched substrates and followed by appropriate mathematical modeling was proved to be a powerful tool for studying the compartmentalized cerebral metabolism. Although brain cells have the ability of using several substrates, glucose is well established as the main fuel for cerebral metabolism (Siesjo, 1978). The most determined metabolic rates upon infusion of ^{13}C-enriched glucose include glucose utilization (CMR_{glc}), neuronal, and glial TCA cycles (V_{TCA}), the malate–aspartate shuttle activity (V_x), apparent neurotransmission flux (V_{NT}), i.e., glutamate–glutamine cycle, and glial anaplerotic pyruvate carboxylation (V_{PC}) (e.g., Sibson et al., 1998; Gruetter et al., 2001; Oz et al., 2004; Patel et al., 2005). However, strong debate is continuously generated on the relative values for these metabolic fluxes and how should they be properly determined (Shestov et al., 2007; Uffmann and Gruetter, 2007; Shen et al., 2009). Many assumptions are generally used for *in vivo* determination of metabolic fluxes and concern has been raised on the reliability of estimated fluxes from experiments using ^{13}C-enriched glucose as metabolic tracer (Shestov et al., 2007; Shen et al., 2009).

We tested the hypothesis that high sensitivity and resolution achieved in ^{13}C NMR spectra at 14.1 T leads to increased reliability in detected ^{13}C enrichment time courses and thus allows us to determine accurate metabolic fluxes. In fact, the present data was acquired with high temporal resolution, during approximately 6 h and with low noise level, which are conditions required for accurate flux estimation (Shestov et al., 2007). In addition, although most mathematical models were designed with many unknown metabolic pools, namely for TCA cycle intermediates, a simplification has been proposed and resulted in a mathematical model where flux estimation is mostly dependent on ^{13}C enrichment of measured metabolites (Uffmann and Gruetter, 2007). The comparison between these two approaches was now performed. For the first time we show experimental evidence supporting that TCA cycle intermediates are not required in mathematical models of cerebral metabolism, as previously suggested by mathematical simulations (Uffmann and Gruetter, 2007).

In this study, metabolic fluxes were determined with higher precision than in previous ^{13}C NMR studies in the brain of rodents (e.g., Choi et al., 2002; Patel et al., 2005) or humans (e.g., Gruetter et al., 2001), as depicted by an average associated error of 8%. We identified substantial pyruvate carboxylation and glial TCA cycle rates that together accounted for more than half of neuronal V_{TCA}, suggesting high glial oxidative metabolism.

MATERIALS AND METHODS

ANIMALS

All experimental procedures involving animals were approved by the local ethics committee. Male Sprague-Dawley rats (276 ± 11 g, $n = 5$, obtained from Charles River Laboratoires, France) were prepared as previously described (Duarte et al., 2009a). Briefly, after fasting for 6 h, rats were anesthetized using 2% isoflurane (Attane, Minrad, NY, USA) in 30% oxygen in air, and then intubated with an endotracheal catheter and ventilated with a pressure-driven ventilator (MRI-1, CWE incorporated, PA, USA). Catheters were inserted into a femoral artery for monitoring blood gases, glucose, lactate, and arterial blood pressure, and into a femoral vein for infusion of saline solutions containing α-chloralose (Acros Organics, Geel, Belgium) or [1,6-^{13}C]glucose (Isotec, Sigma-Aldrich, Basel, Switzerland).

Animals were immobilized in a homebuilt holder with a bite bar and two ear inserts to minimize potential motion. Body temperature was maintained between 37.0 and 37.5°C with a warm water circulation system based on the feedback obtained from a homebuilt rectal temperature probe. Arterial blood pressure, heart rate, and respiratory rate were continuously monitored with an animal monitoring system (SA Instruments, NY, USA). Before inserting the animal in the bore of the magnet, anesthesia was switched to α-chloralose (intravenous bolus of 80 mg/kg and continuous infusion rate of 28 mg/kg/h). Arterial pH and pressures of O_2 and CO_2 were measured using a blood gas analyzer (AVL Compact 3, Diamond Diagnostics, MA, USA). Plasma glucose and lactate concentrations were quantified with the glucose or lactate oxidase methods, respectively, using two multi-assay analyzers (GW7 Micro-Stat, Analox Instruments, London, UK).

The glucose infusion procedure was adapted from the protocol described by Henry et al. (2003a). Briefly, a bolus of 99.9% enriched [1,6-^{13}C]glucose (1.1 M in saline solution) was given at a 5-min exponential decay based on the measured basal glycemia and aiming at 70% plasma fractional enrichment (FE). After the bolus, 70% enriched [1,6-^{13}C]glucose (1.1 M in saline solution) was infused at a rate equivalent to the whole body glucose disposal rate of 33.2 mg/kg/min (Jucker et al., 2002) and adjusted based on concomitantly measured arterial plasma glucose concentrations. Plasma samples were stored at −80°C for determination of substrate FE. Arterial pH and blood gases were maintained within the normal physiological range by adjusting respiratory rate and volume.

IN VIVO NMR SPECTROSCOPY

All *in vivo* NMR experiments were carried out in a DirectDrive spectrometer (Varian, Palo Alto, CA, USA) interfaced to a 14.1 T magnet with a 26-cm horizontal bore (Magnex Scientific, Abingdon, UK), using a homebuilt coil consisting of a ^{1}H quadrature surface coil and a ^{13}C linearly polarized surface coil. The rat brain was positioned in the isocenter of the magnet and fast-spin-echo images with repetition time of 5 s, echo time of 52 ms and echo train length of eight allowed to identify anatomical landmarks, which were used to place the volume of interest (VOI) of 320 μL in the brain. Shimming was performed with FAST(EST)MAP (Gruetter and Tkác, 2000). Localized ^{1}H NMR spectra were acquired using SPECIAL (Mlynárik et al., 2006) with echo time of 2.8 ms and repetition time of 4 s. ^{13}C NMR spectra were acquired using semi-adiabatic distortionless enhancement by polarization transfer (DEPT) combined with 3D-ISIS ^{1}H localization (Henry et al., 2003a).

Spectral analysis was carried out using LCModel (Stephen Provencher Inc., Oakville, ON, Canada) for both ^{1}H (Mlynárik et al., 2006) and ^{13}C NMR spectra (Henry et al., 2003b). Simulation of basis spectra for the observable isotopomers was performed in Matlab (The MathWorks, Natick, MA, USA) as described by Henry et al. (2003b). The scaling of dynamically measured ^{13}C concentrations was based on the FE of glutamate C3, which was determined through the multiplicity of glutamate C4, and the total

glutamate concentration obtained from ^{1}H NMR spectra. In other words, FE of glutamate C3 was determined from the C4 resonance in ^{13}C spectra from the last 20 min, assuming steady-state for C4 enrichment and FE(C3) = C4D34/(C4S + C4D34). Then, relative intensities in ^{13}C NMR spectra were used to scale ^{13}C concentration for all carbon resonances through all time courses. Additionally, *in vitro* ^{13}C NMR spectra from brain extracts and standard solutions including the metabolites of interest allowed correcting for the relative differences in signal enhancement by polarization transfer in DEPT.

IN VITRO NMR SPECTROSCOPY

After each experiment, rats were sacrificed using a focused microwave fixation device (Gerling Applied Engineering, Inc., Modesto, CA, USA) at 4 kW for 2 s. Brain tissue excluding cerebellum was immediately stored at −80°C until extraction. Water-soluble metabolites from brain and plasma samples were extracted with 7% (v/v) perchloric acid (PCA) as previously described (Duarte et al., 2007) and dried with a sample concentrator (Speed-Vac DNA 120, Thermo Fisher Scientific, Wohlen, Switzerland). The dried extracts were dissolved in $^{2}H_2O$ (99.9% ^{2}H, Sigma-Aldrich) and 1.2 mmol sodium fumarate (Sigma-Aldrich) was added as internal standard for quantification by ^{1}H NMR spectroscopy. ^{1}H and ^{13}C NMR spectra were acquired on a 14.1 T DRX-600 spectrometer equipped with a 5-mm cryoprobe (Bruker BioSpin SA, Fallanden, Switzerland) as previously described (Duarte et al., 2007). Peak areas were quantified by curve fitting.

DETERMINATION OF METABOLIC FLUXES

Kinetic modeling of [1,6-^{13}C]glucose metabolism was performed with basis on the mathematical model of compartmentalized cerebral metabolism described by Gruetter et al. (2001). **Figure 1** depicts metabolic pools and fluxes defined in our model, which is detailed in Section "Appendix." An alternative model was designed to eliminate the non-measurable ^{13}C enrichment of TCA cycle intermediates (Uffmann and Gruetter, 2007).

Each model was fitted to the ^{13}C enrichment curves over time using the Levenberg–Marquardt algorithm for non-linear regression, coupled to a Runge–Kutta method for non-stiff systems to obtain numerical solutions of the ordinary differential equations (see Appendix). Significance of the fitted parameters (fluxes) was inferred from t-statistics. F-statistics was used for assessment of fit quality and for inter-model comparison. Reliability of determined fluxes was evaluated by Monte-Carlo analysis, in which Gaussian noise with the same variance of fit residuals was added to the best fit and initial conditions were randomly generated within confidence interval of the obtained value. Typically, 500 simulated datasets were created for each individual analysis. All numerical procedures were performed in Matlab.

The estimated metabolic fluxes are shown as mean ± SD, being the SD resulting from Monte-Carlo simulations. Other results are shown as mean ± SEM of $n = 5$ experiments.

RESULTS

The specific protocol of ^{13}C-enriched glucose infusion raised plasma glucose from 100 to 350 mg/dL in 5 min and then remained constant (**Figure 2A**), leading to a step function in plasma glucose FE of ∼70% (**Figure 2B**). Concentration of lactate in plasma varied during the experiment as consequence of the variable glucose infusion rate that aimed at a stable plasma glucose level (**Figure 2A**). FE of lactate increased at the onset of [1,6-^{13}C]glucose and was maintained constant over time (**Figure 2B**), and may contribute to brain metabolism. For example, at the end of the experiment, the FE of plasma glucose and lactate were 0.67 ± 0.01 and 0.50 ± 0.01, respectively. FE in plasma alanine and acetate increased over the experimental time course and seemed to reach a steady-state after 300 min, respectively achieving a FE of 0.45 ± 0.02 and 0.33 ± 0.01 (**Figure 2C**). Therefore, the influx of ^{13}C labeling from extra-cerebral lactate and acetate was included in the model (see Appendix). Plasma alanine was considered to have minor contribution to brain metabolism since it exists at only 11.2 ± 3.2% of lactate concentration (quantified in PCA extracts of plasma samples by *in vitro* NMR spectroscopy). This is further supported by the relative low rate of alanine transport into the brain and contribution to metabolism (Bröer et al., 2007).

The *in vivo* spectral quality achieved at 14.1 T can be appreciated from **Figure 3**. A major improvement was the increased sensitivity relative to lower fields and the full separation of the carbon positions of glutamate and glutamine C3 which was not possible at, for example, 9.4 T (Henry et al., 2003b). The ^{13}C resonances of glucose, glutamate, glutamine, and aspartate were determined with a temporal resolution of 5.3 min (**Figures 3** and **4**). Total concentration of these amino acids was determined *in vivo* and found to be 8.5 ± 0.4 μmol/g for glutamate, 5.1 ± 0.5 μmol/g for glutamine, and 2.4 ± 0.3 μmol/g for aspartate.

In brain extracts, prepared at the end of the experiment, FE was 0.70 ± 0.02 for glucose, 0.53 ± 0.02 for lactate, and 0.54 ± 0.01 for alanine. Therefore, a significant dilution flux V_{out} must occur, leading to different FE in brain glucose and the end products of glycolysis, namely lactate. Lactate homeostasis resides in a balance between production, consumption and exchange between brain parenchyma, and extra-cerebral lactate equivalents. Plasma lactate was labeled at a different enrichment than that of plasma glucose (**Figure 2**), thus contributing to brain lactate through V_{in}. However, the redundancy between contributions of [1,6-^{13}C]glucose and [3-^{13}C]lactate enriched at different levels to metabolism in mitochondria leads to a high correlation between V_{out}, glucose transport (T_{max}), and consumption (CMR_{glc}) (**Figure 5**). Therefore, glucose transport was determined from the experimental data with a dynamic version of the reversible Michaelis–Menten model described by Duarte et al. (2009b) and transport parameters used to simulate glucose transport that feeds the pyruvate pool: $T_{max} = 0.91 \pm 0.03$ μmol/g/min, $CMR_{glc} = 0.50 \pm 0.02$ μmol/g/min, and $K_t = 0.32 \pm 0.10$ mM. The constraint of parameters directly involved in glucose homeostasis was devoid of significant effects on the remaining metabolic fluxes, with the obvious exception of V_{out}.

The compartmentalized model of brain metabolism previously proposed (Gruetter et al., 2001) was adapted to include a non-zero concentration of aspartate in the glial compartment and a dilution factor at the level of glial acetyl-CoA (see Appendix). Non-linear regression of the model to the determined ^{13}C enrichment curves is shown in **Figure 4**. Following the suggestion that TCA cycle intermediates can be excluded from the mathematical model, at least for the non-compartmentalized case (Uffmann and

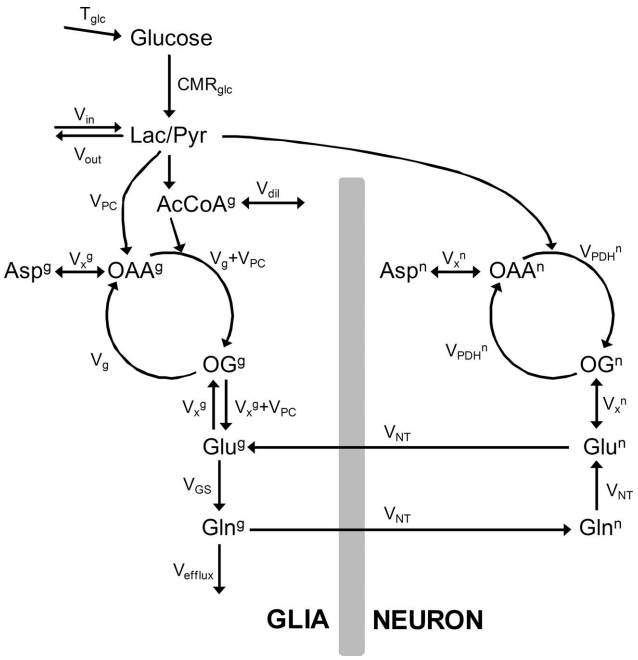

FIGURE 1 | Model of compartmentalized brain metabolism adapted from Gruetter et al. (2001). Glucose transport is here represented by T_{glc}. CMR_{glc} is the cerebral metabolic rate of glucose. Pyruvate (Pyr) originated from glucose consumption is in fast equilibrium with lactate (Lac) that is exchanged between neurons and glia and is diluted with extra-cerebral lactate through V_{out}/V_{in}. V^n_{PDH} is the neuronal TCA cycle, $V_g + V_{PC}$ is the total glial TCA cycle, V_{PC} is the rate of pyruvate carboxylase. In the glial compartment, the dilution of label at the level of acetyl-CoA (AcCoA) by glial specific substrates is accounted by V_{dil}. TCA cycle intermediates oxaloacetate (OAA) and 2-oxoglutarate (OG) exchange with aminoacids through the exchange flux V_X. The apparent glutamatergic neurotransmission (i.e., glutamate–glutamine cycle) is V_{NT} and glutamine synthetase rate is V_{GS}. Finally, efflux of labeling from the metabolic system occurs through the rate of glial glutamine loss V_{efflux}. The superscripts g and n distinguish metabolic pools or fluxes in the glial and neuronal compartments, respectively.

Gruetter, 2007), we further tested the fit of such model (derived in Appendix) with successful results. In any of the cases, the non-linear regressions were performed without imposing any constraint to the eight fluxes of intermediary metabolism that were estimated. Precision of the estimated fluxes was determined by Monte-Carlo simulations and the resulting probability was fitted with a gamma function that, for all estimated fluxes, approached a Gaussian distribution. For the sake of comparison, estimated fluxes with both models are shown in **Table 1**. As the increasing number of experimental ^{13}C enrichment time courses used in the fitting process may increase the accuracy of estimated fluxes, as suggested by numerical simulations (Shestov et al., 2007), we fitted both models providing or not the aspartate C2 and C3 turnover curves (**Table 1**). Although increased precision was found to be associated with the number of fitted ^{13}C enrichment curves, estimated fluxes did not diverge significantly.

For the most complete model, i.e., including TCA cycle intermediates and fitted to ^{13}C enrichment curves of glutamate, glutamine, and aspartate, the TCA cycle V_{TCA} was 0.45 ± 0.01 μmol/g/min and 0.28 ± 0.02 μmol/g/min the neuronal and glial compartments, respectively. Notably, the flux though the malate–aspartate shuttle V_x was in the same order of V_{TCA}. Pyruvate carboxylation V_{PC} was 0.069 ± 0.004 μmol/g/min, accounting for specific labeling of glutamate and glutamine C2. The neurotransmission flux V_{NT} of 0.11 ± 0.01 μmol/g/min is, in our model, the responsible for labeling exchange between the two compartments. These fluxes were not statistically different between the different analyses (**Table 1**).

DISCUSSION

Compartmentalized brain energy metabolism was determined following infusion of [1,6-^{13}C]glucose and direct detection of ^{13}C enrichment of brain metabolites by high resolution ^{13}C NMR spectroscopy at 14.1 T. High sensitivity was achieved in this study and permitted to quantify ^{13}C enrichment curves of brain amino acid carbons with high reproducibility and to reliably determine cerebral metabolic fluxes, as indicated by the mean error of 8% associated to the determined fluxes (**Table 1**). For the first time to our knowledge, we used ^{13}C turnover curves determined *in vivo* in the rat brain for all aliphatic carbons of glutamate, glutamine, and aspartate for metabolic modeling, similarly to what was performed for the human brain (Gruetter et al., 2001). This, together with the high temporal resolution and long time course of the detected ^{13}C enrichment, increased the level of precision of the measured metabolic fluxes (Shestov et al., 2007). For the determined metabolic fluxes, although similar results were obtained in the absence or inclusion of aspartate ^{13}C enrichment curves in the fitting process, precision generally increased with the number of used turnover curves, especially

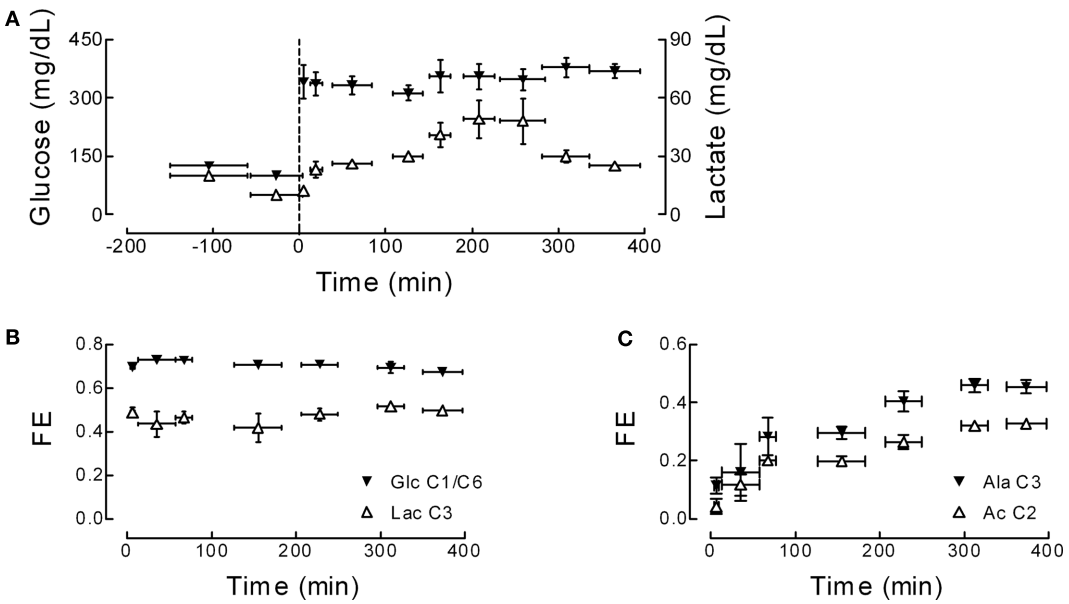

FIGURE 2 | Concentration and fractional enrichment (FE) of plasma glucose, lactate, alanine, and acetate upon infusion of [1,6-^{13}C]glucose. (A) Shows glucose (filled symbols) and lactate (open symbols) concentration determined during the entire time course. **(B)** Depicts FE of glucose and lactate determined by *in vitro* ^{1}H NMR spectroscopy. FE of alternative brain substrates alanine and acetate were determined in ^{1}H NMR spectra of plasma samples **(C)**.

when TCA cycle intermediates are absent from the model (see **Table 1**).

Uffmann and Gruetter (2007) previously demonstrated by means of numerical simulations that the unknown *in vivo* ^{13}C enrichment time courses of TCA cycle intermediates can be neglected using a single compartment model of brain metabolism. We now extended that model to include the two main cerebral metabolic compartments (glial and neuronal compartments) and found similar results in the absence or presence of TCA cycle intermediates in the mathematical model. In fact, similar metabolic fluxes were estimated with the two approaches and identical best fit curves were obtained. However, without the intermediates, increased correlation between the estimated fluxes was observed (**Figure 5**). This is caused by the fact that metabolic fluxes are directly combined in products and quotients in the derived equations.

Recent publications restricted the analysis of cerebral intermediary metabolism by *in vivo* ^{13}C NMR spectroscopy to resonances C4 and C3 and disregarded the C2 of glutamate and glutamine, which may be principally due to low resolution of acquired ^{13}C NMR spectra or to the use of indirect detection of ^{13}C enrichment in ^{1}H NMR spectra (de Graaf et al., 2003; Patel et al., 2010; van Eijsden et al., 2010; Xin et al., 2010). Indirect ^{13}C detection has the great advantage of higher sensitivity but the drawback of lower spectral resolution characteristic of ^{1}H NMR spectroscopy even at 14.1 T (Xin et al., 2010). Our results show that, with increased sensitivity at high magnetic field strengths, direct ^{13}C detection may be preferred. We achieved good time resolution for aliphatic carbons of glutamate and glutamine (the most concentrated metabolites appearing in the ^{13}C spectra of the brain) with high reproducibility between all animals studied. The data further suggested that we could reduce the time span of C4 enrichment curves of these amino acids to 3 min without losing the consistency of the ^{13}C time course measurement (data not shown). Conversely, the ^{13}C enrichment curves could be acquired from a volume of interest smaller than 320 μL (used in this study). In our experimental conditions, we determined the turnover curves for all aliphatic carbons of glutamate, glutamine, and aspartate and provided them for the non-linear fit of the mathematical model (**Figure 4**).

The simultaneous determination of ^{13}C-enriched glucose concentrations in plasma and brain allows measuring glucose transport. Notably, high correlation was found between glucose transport (T_{max}), consumption (CMR_{glc}), and label exchange before mitochondrial oxidation (V_{out}). Therefore, glucose transport was analyzed as described by Duarte et al. (2009b) and the obtained parameters were used to simulate brain glucose enrichment and concentration as input for the metabolic model. However, by simulating T_{max} and CMR_{glc}, correlation between V_{out} and other fluxes increased. V_{out}, along with V_{in}, represent metabolic exchange with other metabolites fueling brain metabolism, such as free amino acids (e.g., Bröer et al., 2007; Boumezbeur et al., 2010), and interaction of glycolysis with other brain pathways like the pentose phosphate shunt (e.g., Dusick et al., 2007). In fact, the brain is capable of lactate uptake and metabolism (e.g., Dienel and Cruz, 2009; Gallagher et al., 2009; Boumezbeur et al., 2010). Exchange between extra-cerebral lactate with pyruvate is modeled by V_{in} and V_{out} and a net gain or loss of lactate concentration is taken into account by the ratio of V_{in} to V_{out}. FE of brain lactate was significantly lower than that of the precursor glucose. Assuming that lactate is in fast exchange with the direct end product of glycolysis, pyruvate, and thus achieves similar FE, there would be a significant diversion of labeling between glucose entry in the brain

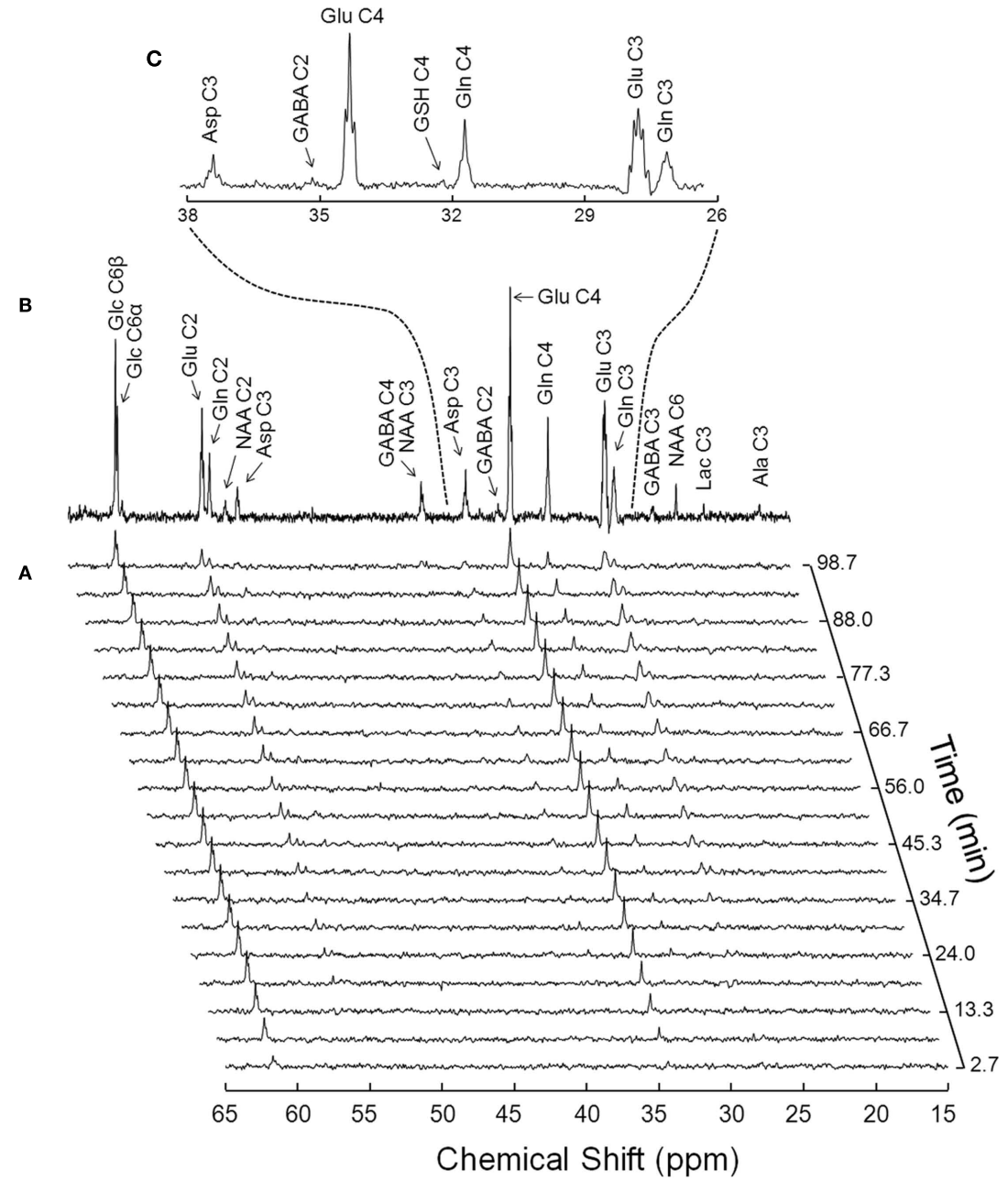

FIGURE 3 | Typical *in vivo* ^{13}C NMR spectra acquired at 14.1 T from a 320-μL volume in the rat brain upon infusion of [1,6-^{13}C]glucose. **(A)** Shows the initial 100 min of a time course of ^{13}C enrichment of brain metabolites from plasma [1,6-^{13}C]glucose, with a temporal resolution of 5.3 min (128 scans with TR of 2.5 s). The spectrum in **(B)** was acquired for 1.8 h, starting 3.5 h after the onset of [1,6-^{13}C]glucose infusion. **(C)** Depicts the expansion of **(B)** from 26 to 38 ppm, where are visible the multiplets originated by the different isotopomers of glutamine (Gln), glutamate (Glu), and aspartate (Asp). For resolution enhancement, Lorentzian–Gaussian apodization was applied before Fourrier transformation [lb = 7, sb = 0.12, and sbs = 0.02 for **(A)**; sb = 0.12 and sbs = 0.02 for **(B,C)**].

and oxidation in the mitochondrial TCA cycle. In fact, a significant V_{out} was determined and, additionally, it was different from V_{in} that represents lactate utilization from extra-cerebral sources (note that plasma lactate was also enriched). Since $V_{out} > V_{in}$, not all glucose consumption rate (CMR_{glc}) follows complete oxidation, i.e. $CMR_{glc(ox)}$. Our results indicate that only 78 ± 4% of the total glucose phosphorylation is oxidized in the TCA cycle, which is comparable to previous findings (discussed in Siesjo, 1978; Dienel and Hertz, 2001).

Different relative FE was observed in carbons of glutamate relative to glutamine. For example, at the end of the experiment, while glutamate C2 enrichment approaches that of C3

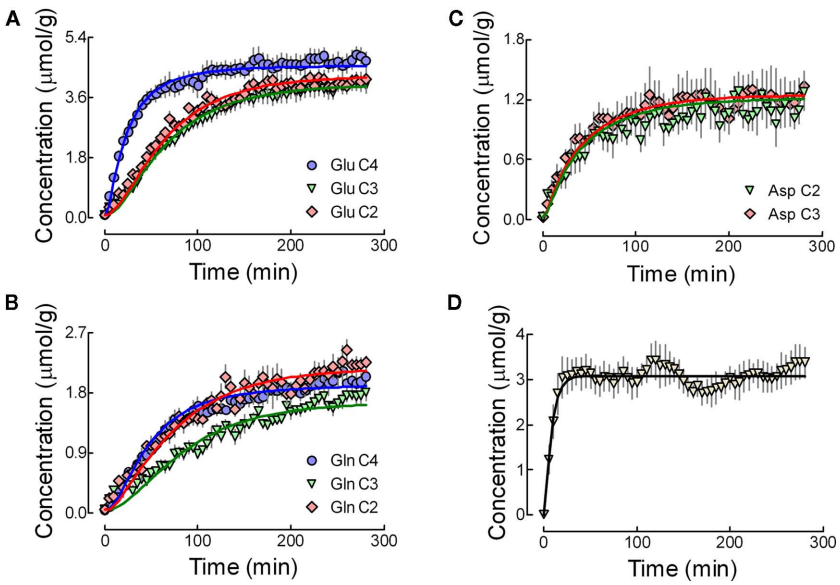

FIGURE 4 | Concentration of enriched glutamate (A), glutamine (B), and aspartate (C) carbons detected *in vivo* during infusion of [1,6-^{13}C]glucose. For glutamate and glutamine, blue, green, and red lines represent best fit to the ^{13}C enrichment curves for C4, C3, and C2, respectively. For aspartate, green and red lines depict C2 and C3. Exact overlap was observed for the best fit curves with both metabolic models, i.e., with and without the inclusion of TCA cycle intermediates. This particular fits were performed with the inclusion of aspartate resonances. Although some experiments were conducted over a longer period (**Figure 2**), the data used for flux estimation was averaged for 280 min. **(D)** Shows the concentration of glucose C6 determined *in vivo* and the fit result of the dynamic reversible Michaelis–Menten model described in Duarte et al. (2009b).

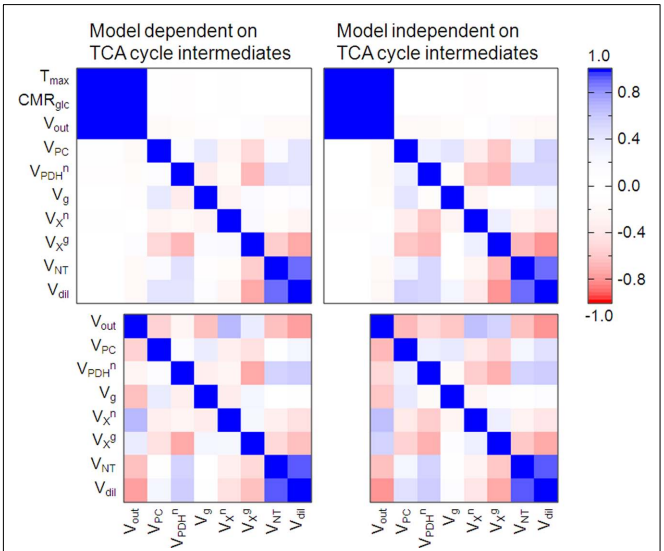

FIGURE 5 | Correlation matrices showing the covariances between estimated metabolic fluxes. Metabolic modeling was performed with all measurable ^{13}C enrichment curves for glutamate, glutamine, and aspartate either including (left plots) or excluding (right plots) TCA cycle intermediate pools. Due to high correlation found between T_{max}, CMR_{glc}, and V_{out}, glucose transport kinetics was then determined as described in Duarte et al. (2009b) and simulated in the present model (bottom matrices).

(**Figure 4A**), glutamine C2 is close to C4 and different from that of C3 (**Figure 4B**). This would only be possible if, in addition to the glial V_{PC} labeling C2 of glutamate and glutamine, the TCA cycle precursor pools in glial and neuronal compartments display different FE. This is consistent with alternative glial specific substrates fueling brain metabolism, namely acetate (Badar-Goffer et al., 1990; Cerdán et al., 1990), fatty acids (Ebert et al., 2003), and ketone bodies (Künnecke et al., 1993), which are oxidized to glial acetyl-CoA. Therefore, a dilution factor was introduced at the level of glial acetyl-CoA (V_{dil}). V_{dil} not only acts as dilution factor for glial acetyl-CoA but can also incorporate ^{13}C label from blood-born acetate (**Figure 2C**, which was considerable at the end of the experiment (FE = 0.33 ± 0.01). This dilution factor also accounts for eventual glial specific metabolic processes that deviate ^{13}C labeling from oxidation in the TCA cycle, such as glycogen synthesis (Gruetter, 2003). V_{dil} was thus found to be slightly higher but not substantially different from the acetate consumption rate determined in the rat brain upon with infusions of ^{13}C enriched acetate (Deelchand et al., 2009). This glial labeling dilution of the acetyl-CoA pool through V_{dil} was positively correlated to the apparent neurotransmission V_{NT} as they are both responsible for the observed difference in C4 labeling between glutamate and glutamine.

One should note that, since glutamine and glutamate are mostly located in glial cells and neurons, respectively, V_{dil} also accounts for the ^{13}C labeling dilution between the two amino acids. Because part of glutamine may be undetected in *in vivo* ^{1}H NMR spectra (e.g., Hancu and Port, 2011), we determined total glutamine relative to that of glutamate using resonance intensities and FEs from the ^{13}C NMR spectra. Therefore, a total glutamine concentration different from 5.1 ± 0.5 μmol/g (measured in this study), may lead to a modification of V_{dil}.

Table 1 | Cerebral metabolic fluxes (in μmol/g/min) determined either including or excluding TCA cycle intermediates.

Curves fitted	With TCA cycle intermediates		Without TCA cycle intermediates	
	Glu + Gln	Glu + Gln + Asp	Glu + Gln	Glu + Gln + Asp
DETERMINED FLUXES				
V_{out}	0.36 ± 0.05	0.42 ± 0.04	0.37 ± 0.06	0.41 ± 0.05
V_{PC}	0.070 ± 0.004	0.069 ± 0.004	0.069 ± 0.005	0.067 ± 0.004
V^n_{PDH}	0.44 ± 0.01	0.45 ± 0.01	0.46 ± 0.02	0.46 ± 0.01
V_g	0.23 ± 0.02	0.21 ± 0.02	0.23 ± 0.03	0.21 ± 0.02
V^n_X	0.76 ± 0.07	0.91 ± 0.09	0.83 ± 0.11	0.99 ± 0.12
V^g_X	0.17 ± 0.06	0.16 ± 0.05	0.23 ± 0.12	0.25 ± 0.16
V_{NT}	0.12 ± 0.01	0.11 ± 0.01	0.11 ± 0.01	0.10 ± 0.01
V_{dil}	0.76 ± 0.15	0.66 ± 0.10	0.64 ± 0.13	0.55 ± 0.08
CALCULATED FLUXES				
V^g_{TCA}	0.30 ± 0.02	0.28 ± 0.02	0.30 ± 0.03	0.27 ± 0.02
V_{in}	0.19 ± 0.05	0.22 ± 0.05	0.21 ± 0.07	0.24 ± 0.05
V_{GS}	0.19 ± 0.01	0.18 ± 0.01	0.18 ± 0.01	0.17 ± 0.01
$CMR_{glc(ox)}$	0.41 ± 0.02	0.39 ± 0.02	0.42 ± 0.04	0.40 ± 0.02

Determinations were made with ^{13}C enrichment curves from glutamine (Gln), glutamate (Glu), and eventually aspartate (Asp). Estimated values are presented with two significant digits and the associated SD was determined by Monte-Carlo analysis with at least 500 simulations. Calculated fluxes are defined in the Section "Appendix."

The neuronal and glial V_{TCA} were 0.45 ± 0.01 and 0.28 ± 0.02 μmol/g/min, respectively. This means that glial V_{TCA} accounts for 38 ± 3% of total mitochondrial oxidative metabolism, from which 25 ± 1% is V_{PC}. V_{PC} is further increased upon higher cerebral activity in the conscious rat (Oz et al., 2004) and reduced under isoelectricity (Sibson et al., 1998; Choi et al., 2002). This substantial pyruvate carboxylation flux supports the active role of glial cells in their metabolic relationship with neurons, especially during synaptic transmission. In fact, in cultured astrocytes, extracellular potassium was suggested to stimulate bicarbonate influx (Brookes and Turner, 1994), which can induce anaplerosis (Gamberino et al., 1997), and to increase glutamine content (Brookes and Turner, 1993). In our model, V_{GS} results from the addition of V_{PC} to V_{NT} and thus depicts this coupling of anaplerosis to glutamine synthesis, both occurring in the glial compartment. To maintain mass balance in the glutamine–glutamate cycle, exit of labeling from the cycle was modeled as V_{efflux}, representing other fates of glutamate and glutamine (McKenna, 2007). It is proposed that astrocytic glycolysis sustains glutamatergic neurotransmission and the resulting lactate is shuttled to neurons for oxidative metabolism (Pellerin and Magistretti, 1994; Magistretti et al., 1999). This hypothesis considers that astrocytic metabolism is mainly glycolytic, which would be sufficient to meet the energetic requirements of glutamate uptake and glutamine synthesis in the neurotransmission process (Magistretti et al., 1999). However, clearance of glutamate could be fueled by mitochondrial oxidative phosphorylation in astrocytes (Dienel and Hertz, 2001). In accordance, the present results suggest that a substantial part of mitochondrial oxidation of glycolytic pyruvate takes place in the glial compartment, as observed in the conscious rat (Oz et al., 2004).

The exchange between amino acids in the cytosol and the mitochondrial matrix, where the TCA cycle takes place, is mediated by the malate–aspartate shuttle and responsible for most labeling exchange between glutamate or aspartate and their oxo-acids 2-oxoglutarate and oxaloacetate, represented by V_x (Gruetter et al., 2001). V_x has frequently been assumed to be much larger than V_{TCA} (e.g., Hyder et al., 1996, 1997; Sibson et al., 1998), i.e., $V_{TCA}/V_x = 0$, which allows simplification of the mathematical models but may lead to underestimation of TCA cycle fluxes (see Uffmann and Gruetter, 2007). This assumption implies that ^{13}C enrichment of glutamate and aspartate resembles that of OG and OAA, respectively, which may not be accurate (Gruetter et al., 2001). Experimental evidence shows that this flux could be either in the range of the TCA cycle flux (e.g., Gruetter et al., 2001; Oz et al., 2004) or effectively larger (e.g., de Graaf et al., 2004; Yang et al., 2009). In the rat brain under α-chloralose, we determined ^{13}C enrichment curves with increased sensitivity and estimated a finite V_x that is on the same order of V_{TCA} in both neurons and glia. Although from all estimated fluxes, glial V_x was the poorest estimated, i.e., with larger relative SD, all numerical simulations resulted in a V^g_X on the order of V^g_{TCA}. To our knowledge this is the first time that V_x is simultaneously determined in neurons and glia. Half of the total V_{TCA}, that represents oxidative glucose consumption $CMR_{glc(ox)}$, was found to be 0.39 ± 0.02 μmol/g/min (see **Table 1**), in agreement to other determinations by ^{13}C NMR (Henry et al., 2002), or to measurements of CMR_{O2} by ^{17}O NMR spectroscopy (Zhu et al., 2002) and CMR_{glc} by autoradiography (Ueki et al., 1992; Nakao et al., 2001) in rats under α-chloralose anesthesia.

The neurotransmission flux V_{NT} represents the flow of ^{13}C labeling in the glutamate–glutamine cycle and was now determined to be 0.11 ± 0.01 μmol/g/min (see **Table 1**) that is similar to that reported by (Sibson et al., 1998) for the rat brain under α-chloralose anesthesia. It should however be noted that in the present work, V_{NT} was determined with higher precision

as suggested by an SD below 10%. The use of the C2 turnover curves of both glutamate and glutamine greatly contributed to the precision in the estimation of V_{NT} by receiving direct ^{13}C labeling input through pyruvate carboxylation that occurs in the glial compartment. A positive correlation was observed between V_{NT} and the dilution of glial acetyl-CoA V_{dil} (Shen et al., 2009), which resides in the fact that V_{dil} creates a difference between the FEs of glutamine and glutamate while V_{NT} is responsible for its dissipation.

In vitro studies suggest the existence of high fumarase activity randomizing ^{13}C labeling from oxaloacetate (Sonnewald et al., 1993; Merle et al., 1996). Direct injection of [1-^{14}C]pyruvate in the neocortex of mice labels glutamate and glutamine, which would only occur with pyruvate carboxylation and a notable rate through fumarase (Nguyen et al., 2007). In an alternative model, flux through fumarase (V_{fum}) allowing labeling exchange between OAA C3 and C2 was included. V_{fum} was detected but poorly determined, i.e., presented high relative SD, and was not significantly different from zero, as in a previous *in vivo* study (Oz et al., 2004). This is likely due to the high correlation of V_{fum} to V_{PC} that alone accounts for the difference in C2 and C3 enrichment of glutamate and glutamine. The fact that aspartate, which is in exchange with OAA, is mostly located in neurons (discussed in Gruetter et al., 2001), makes it insensitive to this flux. In accordance to the primary location of aspartate to neurons, NMR spectroscopy of brain extracts at the end of the experiment revealed similar FE for C3 and C2 of aspartate in our study (0.52 ± 0.02 and 0.52 ± 0.01, respectively). However, the significant difference between ^{13}C enrichment of carbons C2 and C3 of glutamate and glutamine at steady-state is in agreement with low V_{fum} compared to V_{PC}.

Pyruvate recycling was suggested to occur in the brain (e.g., Cerdán et al., 1990; Sonnewald et al., 1996; Waagepetersen et al., 2002; Serres et al., 2007; Scafidi et al., 2010). This process would lead to enrichment of pyruvate C2 and consequently lactate C2 and, in fact, FE of lactate C2 in brain extracts at the end of the experiment was 0.029 ± 0.001. Although significant compared to the natural abundance of 0.011 ($P < 0.01$ with one-sample t test), it was much lower than the enrichment of C3 and therefore negligible. This pathway was suggested to be mainly used for complete oxidation of glutamate or glutamine in the TCA cycle and to occur in cultured astrocytes but not in neurons and in co-cultures of both (Sonnewald et al., 1996; Waagepetersen et al., 2002). This is in agreement with the lack of evidence for substantial pyruvate recycling *in vivo*. In addition, high glucose concentration may lead to reduction of the pyruvate recycling flux (discussed in Waagepetersen et al., 2002) and some C2 enrichment observed *in vivo* may be of systemic origin due to scrambling of ^{13}C labeling in tissues such as the liver (discussed in Serres et al., 2007).

CONCLUSION

The present work experimentally demonstrates that reliable determination of ^{13}C enrichment curves with high temporal resolution increases the precision of estimated metabolic fluxes. Additionally, precision increases with the number of experimentally measured turnover curves. Furthermore, we provide experimental evidence that non-measurable ^{13}C enrichment of TCA cycle intermediates is not required for flux estimation, but increased correlation between the resulting fluxes must be expected. We found a substantial glial oxidative metabolism, part being driven through pyruvate carboxylase, which corresponds to more than half of the neuronal TCA cycle rate. This is consistent with the active role of astrocytes in the support of glutamatergic neurotransmission.

ACKNOWLEDGMENTS

This work was supported by Swiss National Science Foundation (grant 131087) and by Centre d'Imagerie BioMédicale (CIBM) of the UNIL, UNIGE, HUG, CHUV, EPFL, and the Leenaards and Jeantet Foundations.

REFERENCES

Badar-Goffer, R. S., Bachelard, H. S., and Morris, P. G. (1990). Cerebral metabolism of acetate and glucose studied by 13C-n.m.r. spectroscopy – a technique for investigating metabolic compartmentation in the brain. *Biochem. J.* 266, 133–139.

Boumezbeur, F., Petersen, K. F., Cline, G. W., Mason, G. F., Behar, K. L., Shulman, G. I., and Rothman, D. L. (2010). The contribution of blood lactate to brain energy metabolism in humans measured by dynamic 13C nuclear magnetic resonance spectroscopy. *J. Neurosci.* 30, 13983–13991.

Bröer, S., Bröer, A., Hansen, J. T., Bubb, W. A., Balcar, V. J., Nasrallah, F. A., Garner, B., and Rae, C. (2007). Alanine metabolism, transport, and cycling in the brain. *J. Neurochem.* 102, 1758–1770.

Brookes, N., and Turner, R. J. (1993). Extracellular potassium regulates the glutamine content of astrocytes: mediation by intracellular pH. *Neurosci. Lett.* 160, 73–76.

Brookes, N., and Turner, R. J. (1994). K(()-induced alkalinization in mouse cerebral astrocytes mediated by reversal of electrogenic Na(()-HCO3- cotransport. *Am. J. Physiol.* 267, C1633–C1640.

Cerdán, S., Künnecke, B., and Seelig, J. (1990). Cerebral metabolism of [1,2-13C2]acetate as detected by in vivo and in vitro 13C NMR. *J. Biol. Chem.* 265, 12916–12926.

Choi, I. Y., Lei, H., and Gruetter, R. (2002). Effect of deep pentobarbital anesthesia on neurotransmitter metabolism in vivo: on the correlation of total glucose consumption with glutamatergic action. *J. Cereb. Blood Flow Metab.* 22, 1343–1351.

de Graaf, R. A., Brown, P. B., Mason, G. F., Rothman, D. L., and Behar, K. L. (2003). Detection of [1,6-13C2]-glucose metabolism in rat brain by in vivo 1H-[13C]-NMR spectroscopy. *Magn. Reson. Med.* 49, 37–46.

de Graaf, R. A., Mason, G. F., Patel, A. B., Rothman, D. L., and Behar, K. L. (2004). Regional glucose metabolism and glutamatergic neurotransmission in rat brain in vivo. *Proc. Natl. Acad. Sci. U.S.A.* 101, 12700–12705.

Deelchand, D. K., Shestov, A. A., Koski, D. M., Ugurbil, K., and Henry, P. G. (2009). Acetate transport and utilization in the rat brain. *J. Neurochem.* 109, 46–54.

Dienel, G. A., and Cruz, N. F. (2009). Exchange-mediated dilution of brain lactate specific activity: implications for the origin of glutamate dilution and the contributions of glutamine dilution and other pathways. *J. Neurochem.* 109(Suppl. 1), 30–37.

Dienel, G. A., and Hertz, L. (2001). Glucose and lactate metabolism during brain activation. *J. Neurosci. Res.* 66, 824–838.

Duarte, J. M. N., Carvalho, R. A., Cunha, R. A., and Gruetter, R. (2009a). Caffeine consumption attenuates neurochemical modifications in the hippocampus of streptozotocin-induced diabetic rats. *J. Neurochem.* 111, 368–379.

Duarte, J. M. N., Morgenthaler, F. D., Lei, H., Poitry-Yamate, C., and Gruetter, R. (2009b). Steady-state brain glucose transport kinetics re-evaluated with a four-state conformational model. *Front. Neuroenergetics* 1:6. doi: 10.3389/neuro.14.006.2009

Duarte, J. M. N., Cunha, R. A., and Carvalho, R. A. (2007). Different metabolism of glutamatergic and GABAergic compartments in superfused hippocampal slices characterized by nuclear magnetic resonance spectroscopy. *Neuroscience* 144, 1305–1313.

Dusick, J. R., Glenn, T. C., Lee, W. N., Vespa, P. M., Kelly, D. F., Lee, S. M., Hovda, D. A., and Martin, N. A. (2007). Increased pentose phosphate pathway flux after clinical traumatic brain injury: a [1,2-13C2]glucose labeling study in humans. *J. Cereb. Blood Flow Metab.* 27, 1593–1602.

Ebert, D., Haller, R. G., and Walton, M. E. (2003). Energy contribution of octanoate to intact rat brain metabolism measured by 13C nuclear magnetic resonance spectroscopy. *J. Neurosci.* 23, 5928–5935.

Gallagher, C. N., Carpenter, K. L., Grice, P., Howe, D. J., Mason, A., Timofeev, I., Menon, D. K., Kirkpatrick, P. J., Pickard, J. D., Sutherland, G. R., and Hutchinson, P. J. (2009). The human brain utilizes lactate via the tricarboxylic acid cycle: a 13C-labelled microdialysis and high-resolution nuclear magnetic resonance study. *Brain* 132, 2839–2849.

Gamberino, W. C., Berkich, D. A., Lynch, C. J., Xu, B., and LaNoue, K. F. (1997). Role of pyruvate carboxylase in facilitation of synthesis of glutamate and glutamine in cultured astrocytes. *J. Neurochem.* 69, 2312–2325.

Gjedde, A., and Marrett, S. (2001). Glycolysis in neurons, not astrocytes, delays oxidative metabolism of human visual cortex during sustained checkerboard stimulation in vivo. *J. Cereb. Blood Flow Metab.* 21, 1384–1392.

Gruetter, R. (2003). Glycogen: the forgotten cerebral energy store. *J. Neurosci. Res.* 74, 179–183.

Gruetter, R., Seaquist, E. R., and Ugurbil, K. (2001). A mathematical model of compartmentalized neurotransmitter metabolism in the human brain. *Am. J. Physiol. Endocrinol. Metab.* 281, E100–E112.

Gruetter, R., and Tkác, I. (2000). Field mapping without reference scan using asymmetric echo-planar techniques. *Magn. Reson. Med.* 43, 319–323.

Hancu, I., and Port, J. (2011). The case of the missing glutamine. *NMR. Biomed.* doi: 10.1002/nbm.1620. [Epub ahead of print].

Henry, P. G., Lebon, V., Vaufrey, F., Brouillet, E., Hantraye, P., and Bloch, G. (2002). Decreased TCA cycle rate in the rat brain after acute 3-NP treatment measured by in vivo 1H-13C NMR spectroscopy. *J. Neurochem.* 82, 857–866.

Henry, P. G., Tkác, I., and Gruetter, R. (2003a). 1H-localized broadband 13C NMR spectroscopy of the rat brain in vivo at 9.4 T. *Magn. Reson. Med.* 50, 684–692.

Henry, P. G., Oz, G., Provencher, S., and Gruetter, R. (2003b). Toward dynamic isotopomer analysis in the rat brain in vivo: automatic quantitation of 13C NMR spectra using LCModel. *NMR. Biomed.* 16, 400–412.

Hyder, F., Chase, J. R., Behar, K. L., Mason, G. F., Siddeek, M., Rothman, D. L., and Shulman, R. G. (1996). Increased tricarboxylic acid cycle flux in rat brain during forepaw stimulation detected with 1H[13C]NMR. *Proc. Natl. Acad. Sci. U.S.A.* 93, 7612–7617.

Hyder, F., Rothman, D. L., Mason, G. F., Rangarajan, A., Behar, K. L., and Shulman, R. G. (1997). Oxidative glucose metabolism in rat brain during single forepaw stimulation: a spatially localized 1H[13C] nuclear magnetic resonance study. *J. Cereb. Blood Flow Metab.* 17, 1040–1047.

Jucker, B. M., Schaeffer, T. R., Haimbach, R. E., McIntosh, T. S., Chun, D., Mayer, M., Ohlstein, D. H., Davis, H. M., Smith, S. A., Cobitz, A. R., and Sarkar, S. K. (2002). Normalization of skeletal muscle glycogen synthesis and glycolysis in rosiglitazone-treated Zucker fatty rats: an in vivo nuclear magnetic resonance study. *Diabetes* 51, 2066–2073.

Künnecke, B., Cerdán, S., and Seelig, J. (1993). Cerebral metabolism of [1,2-13C2]glucose and [U-13C4]3-hydroxybutyrate in rat brain as detected by 13C NMR spectroscopy. *NMR Biomed.* 6, 264–277.

Magistretti, P. J., Pellerin, L., Rothman, D. L., and Shulman, R. G. (1999). Energy on demand. *Science* 283, 496–497.

Mangia, S., Simpson, I. A., Vannucci, S. J., and Carruthers, A. (2009). The in vivo neuron-to-astrocyte lactate shuttle in human brain: evidence from modeling of measured lactate levels during visual stimulation. *J. Neurochem.* 109, 55–62.

McKenna, M. C. (2007). The glutamate-glutamine cycle is not stoichiometric: fates of glutamate in brain. *J. Neurosci. Res.* 85, 3347–3358.

Merle, M., Martin, M., Villégier, A., and Canioni, P. (1996). Mathematical modelling of the citric acid cycle for the analysis of glutamine isotopomers from cerebellar astrocytes incubated with [1-13C]glucose. *Eur. J. Biochem.* 239, 742–751.

Mintun, M. A., Vlassenko, A. G., Rundle, M. M., and Raichle, M. E. (2004). Increased lactate/pyruvate ratio augments blood flow in physiologically activated human brain. *Proc. Natl. Acad. Sci. U.S.A.* 101, 659–664.

Mlynárik, V., Gambarota, G., Frenkel, H., and Gruetter, R. (2006). Localized short-echo-time proton MR spectroscopy with full signal-intensity acquisition. *Magn. Reson. Med.* 56, 965–970.

Nakao, Y., Itoh, Y., Kuang, T. Y., Cook, M., Jehle, J., and Sokoloff, L. (2001). Effects of anesthesia on functional activation of cerebral blood flow and metabolism. *Proc. Natl. Acad. Sci. U.S.A.* 98, 7593–7598.

Nguyen, N. H., Morland, C., Gonzalez, S. V., Rise, F., Storm-Mathisen, J., Gundersen, V., and Hassel, B. (2007). Propionate increases neuronal histone acetylation, but is metabolized oxidatively by glia. Relevance for propionic acidemia. *J. Neurochem.* 101, 806–814.

Oz, G., Berkich, D. A., Henry, P. G., Xu, Y., LaNoue, K., Hutson, S. M., and Gruetter, R. (2004). Neuroglial metabolism in the awake rat brain: CO2 fixation increases with brain activity. *J. Neurosci.* 24, 11273–11279.

Patel, A. B., de Graaf, R. A., Mason, G. F., Rothman, D. L., Shulman, R. G., and Behar, K. L. (2005). The contribution of GABA to glutamate/glutamine cycling and energy metabolism in the rat cortex in vivo. *Proc. Natl. Acad. Sci. U.S.A.* 102, 5588–5593.

Patel, A. B., de Graaf, R. A., Rothman, D. L., Behar, K. L., and Mason, G. F. (2010). Evaluation of cerebral acetate transport and metabolic rates in the rat brain in vivo using 1H-[13C]-NMR. *J. Cereb. Blood Flow Metab.* 30, 1200–1213.

Pellerin, L., and Magistretti, P. J. (1994). Glutamate uptake into astrocytes stimulates aerobic glycolysis: a mechanism coupling neuronal activity to glucose utilization. *Proc. Natl. Acad. Sci. U.S.A.* 91, 10625–10629.

Scafidi, S., Fiskum, G., Lindauer, S. L., Bamford, P., Shi, D., Hopkins, I., and McKenna, M. C. (2010). Metabolism of acetyl-L-carnitine for energy and neurotransmitter synthesis in the immature rat brain. *J. Neurochem.* 114, 820–831.

Serres, S., Bezancon, E., Franconi, J. M., and Merle, M. (2007). Brain pyruvate recycling and peripheral metabolism: an NMR analysis ex vivo of acetate and glucose metabolism in the rat. *J. Neurochem.* 101, 1428–1440.

Shen, J., Rothman, D. L., Behar, K. L., and Xu, S. (2009). Determination of the glutamate-glutamine cycling flux using two-compartment dynamic metabolic modeling is sensitive to astroglial dilution. *J. Cereb. Blood Flow Metab.* 29, 108–118.

Shestov, A. A., Valette, J., Ugurbil, K., and Henry, P. G. (2007). On the reliability of 13C metabolic modeling with two-compartment neuronal-glial models. *J. Neurosci. Res.* 85, 3294–3303.

Shulman, R. G., Hyder, F., and Rothman, D. L. (2003). Cerebral metabolism and consciousness. *C. R. Biol.* 326, 253–273.

Sibson, N. R., Dhankhar, A., Mason, G. F., Rothman, D. L., Behar, K. L., and Shulman, R. G. (1998). Stoichiometric coupling of brain glucose metabolism and glutamatergic neuronal activity. *Proc. Natl. Acad. Sci. U.S.A.* 95, 316–321.

Siesjo, B. K. (1978). *Brain Energy Metabolism*. New York: Wiley, 101–130.

Simpson, I. A., Carruthers, A., and Vannucci, S. J. (2007). Supply and demand in cerebral energy metabolism: the role of nutrient transporters. *J. Cereb. Blood Flow Metab.* 27, 1766–1791.

Sonnewald, U., Westergaard, N., Hassel, B., Müller, T. B., Unsgård, G., Fonnum, F., Hertz, L., Schousboe, A., and Petersen, S. B. (1993). NMR spectroscopic studies of 13C acetate and 13C glucose metabolism in neocortical astrocytes: evidence for mitochondrial heterogeneity. *Dev. Neurosci.* 15, 351–358.

Sonnewald, U., Westergaard, N., Jones, P., Taylor, A., Bachelard, H. S., and Schousboe, A. (1996). Metabolism of [U-13C5] glutamine in cultured astrocytes studied by NMR spectroscopy: first evidence of astrocytic pyruvate recycling. *J. Neurochem.* 67, 2566–2572.

Ueki, M., Mies, G., and Hossmann, K. A. (1992). Effect of alpha-chloralose, halothane, pentobarbital and nitrous oxide anesthesia on metabolic coupling in somatosensory cortex of rat. *Acta Anaesthesiol. Scand.* 36, 318–322.

Uffmann, K., and Gruetter, R. (2007). Mathematical modeling of 13C label incorporation of the TCA cycle: the concept of composite precursor function. *J. Neurosci. Res.* 85, 3304–3317.

van Eijsden, P., Behar, K. L., Mason, G. F., Braun, K. P., and de Graaf, R. A. (2010). In vivo neurochemical profiling of rat brain by 1H-[13C] NMR spectroscopy: cerebral energetics and glutamatergic/GABAergic

neurotransmission. *J. Neurochem.* 112, 24–33.

Waagepetersen, H. S., Qu, H., Hertz, L., Sonnewald, U., and Schousboe, A. (2002). Demonstration of pyruvate recycling in primary cultures of neocortical astrocytes but not in neurons. *Neurochem. Res.* 27, 1431–1437.

Xin, L., Mlynárik, V., Lanz, B., Frenkel, H., and Gruetter, R. (2010). 1H-[13C] NMR spectroscopy of the rat brain during infusion of [2-13C] acetate at 14.1 T. *Magn. Reson. Med.* 64, 334–340.

Yang, J., Xu, S., and Shen, J. (2009). Fast isotopic exchange between mitochondria and cytosol in brain revealed by relayed 13C magnetization transfer spectroscopy. *J. Cereb. Blood Flow Metab.* 29, 661–669.

Zhu, X. H., Zhang, Y., Tian, R. X., Lei, H., Zhang, N., Zhang, X., Merkle, H., Ugurbil, K., and Chen, W. (2002). Development of 17O NMR approach for fast imaging of cerebral metabolic rate of oxygen in rat brain at high field. *Proc. Natl. Acad. Sci. U.S.A.* 99, 13194–13199.

Zwingmann, C., and Leibfritz, D. (2003). Regulation of glial metabolism studied by 13C-NMR. *NMR Biomed.* 16, 370–399.

Conflict of Interest Statement: The authors declare that the research was conducted in the absence of any commercial or financial relationships that could be construed as a potential conflict of interest.

Received: 01 April 2011; accepted: 17 May 2011; published online: 06 June 2011.

Citation: Duarte JMN, Lanz B and Gruetter R (2011) Compartmentalized cerebral metabolism of [1,6-^{13}C]glucose determined by in vivo ^{13}C NMR spectroscopy at 14.1 T. Front. Neuroenerg. ***3****:3. doi: 10.3389/fnene.2011.00003*

APPENDIX

KINETIC MODEL OF [1,6-^{13}C]GLUCOSE METABOLISM

The mathematical model of compartmentalized cerebral metabolism was adapted from Gruetter et al. (2001) and this publication should be consulted for an exhaustive description of the model. In **Figure 1** are depicted the metabolic pools and fluxes in glia and neurons used to define the model.

Metabolic but not isotopic steady-state was assumed over the time course of [1,6-^{13}C]glucose infusion. Metabolite concentrations determined *in vivo* (all in μmol/g) were 8.5 ± 0.4 for glutamate, 5.1 ± 0.5 for glutamine, and 2.4 ± 0.3 for aspartate. The remaining concentrations required for the model were assumed. Acetyl-CoA and TCA cycle intermediates were considered to be 0.1 μmol/g in both compartments. Pyruvate was assumed to occur at 10% of lactate concentration (e.g., Mintun et al., 2004) that was measured as 0.7 ± 0.1 μmol/g. Neurons were assumed to retain 90% of total glutamate and aspartate pools, while glial cells contain 90% of total observed glutamine concentration. Due to fast exchange between the two compartments, a single virtual pool of pyruvate was considered to be shared by neurons and glia. This also implies that isotopic enrichment in pyruvate is equivalent to lactate, which is detectable.

At metabolic steady-state, the fraction of glucose oxidation entering the TCA cycle is $(V_{\mathrm{TCA}}^{\mathrm{n}} + V_{\mathrm{TCA}}^{\mathrm{g}} + V_{\mathrm{PC}})/2$ that we call $\mathrm{CMR_{glc(ox)}}$. Similarly, total glucose consumption ($\mathrm{CMR_{glc}}$) is $\mathrm{CMR_{glc(ox)}} + (V_{\mathrm{out}} - V_{\mathrm{in}})/2$. When the outflow ($V_{\mathrm{out}}$) of labeling at the level of lactate equals the inflow (V_{in}) from extra-cerebral lactate, the total glucose consumption is used for oxidation in the TCA cycle.

The TCA cycle was considered equivalent to the flux through pyruvate dehydrogenase. While in the neuron $V_{\mathrm{TCA}}^{\mathrm{n}}$ equals $V_{\mathrm{PDH}}^{\mathrm{n}}$, in the glia $V_{\mathrm{TCA}}^{\mathrm{g}}$ is $V_{\mathrm{g}} + V_{\mathrm{PC}}$, corresponding to the total oxidation of one molecule of pyruvate.

The flux through neuronal glutaminase is V_{NT}. In the glia, glutaminase was neglected because the net flux of ^{13}C follows the direction of the apparent neurotransmission cycle V_{NT}. The net loss of ^{13}C labeling was modeled as V_{efflux} and mass conservation sets it equivalent to the anaplerotic flux through pyruvate carboxylase V_{PC}. Thus $V_{\mathrm{GS}} = V_{\mathrm{NT}} + V_{\mathrm{PC}}$.

Glucose transport across the BBB was defined using a reversible Michaelis–Menten kinetics as previously described for the rat brain (Duarte et al., 2009b). Therefore, brain glucose ($\mathrm{G_{brain}}$) is given by the following expression:

$$\frac{\mathrm{dG_{brain}}}{\mathrm{dt}} = T_{\max}\frac{\mathrm{G_{plasma}}(t) - \mathrm{G_{brain}}(t)/V_{\mathrm{d}}}{K_{\mathrm{t}} + \mathrm{G_{brain}}(t)/V_{\mathrm{d}} + \mathrm{G_{plasma}}(t)} - \mathrm{CMR_{glc}}$$

where $T_{\max}$ is the apparent maximal transport rate, K_{t} is the apparent Michaelis constant for glucose transport, $\mathrm{CMR_{glc}}$ is the cerebral metabolic rate of glucose consumption, and V_{d} is the physical volume for glucose distribution in the brain (0.77 mL/g, as in Duarte et al., 2009b). Similarly, for ^{13}C-enriched carbons of glucose, transport is defined by

$$\frac{\mathrm{d}^{13}\mathrm{G_{brain}}}{\mathrm{dt}} = T_{\max}\frac{^{13}\mathrm{G_{plasma}}(t) - {}^{13}\mathrm{G_{brain}}(t)/V_{\mathrm{d}}}{K_{\mathrm{t}} + \mathrm{G_{brain}}(t)/V_{\mathrm{d}} + \mathrm{G_{plasma}}(t)} - \mathrm{CMR_{glc}}\frac{^{13}\mathrm{G_{brain}}(t)}{\mathrm{G_{brain}}(t)}.$$

Although brain glucose can divert to other pathways, it is consumed mainly through glycolysis and the ^{13}C enrichment in C1 and C6 originates the C3 of pyruvate. Pyruvate was considered to be in fast equilibrium with lactate that is exchanged between compartments and thus a single pyruvate pool was assumed in the model (**Figure 1**). Brain pyruvate enrichment is defined as follows:

$$\frac{\mathrm{d}^{13}\mathrm{Pyr_3}}{\mathrm{dt}} = \mathrm{CMR_{glc}}\left(\frac{^{13}\mathrm{Glc_1}(t) + {}^{13}\mathrm{Glc_6}(t)}{\mathrm{Glc}(t)}\right) + V_{\mathrm{in}}\frac{^{13}\mathrm{Lac_3}(t)}{\mathrm{Lac}(t)} - \left(V_{\mathrm{out}} + V_{\mathrm{TCA}}^{\mathrm{n}} + V_{\mathrm{TCA}}^{\mathrm{g}} + V_{\mathrm{PC}}\right)\frac{^{13}\mathrm{Pyr_3}(t)}{\mathrm{Pyr}}$$

Note that, in the model, total concentration of extra-cerebral lactate (Lac) may vary over time in accordance to the observed plasma lactate levels (**Figure 2**). Transport of lactate into the brain was simulated with a reversible Michaelis–Menten kinetics as described by Boumezbeur et al. (2010) leading to enrichment of ^{13}Lac from plasma lactate. Therefore, alteration of plasma lactate levels is reflected in brain lactate concentration. However, total concentration of pyruvate remains invariable because V_{in} is constant under the assumption of metabolic steady-state.

In peripheral tissues, metabolism of [1,6-^{13}C]glucose produces [3-^{13}C]lactate that is released to the blood stream. Incorporation of ^{13}C from blood-born lactate ($\mathrm{Lac_3}$) into brain metabolism may occur (e.g., Dienel and Cruz, 2009; Gallagher et al., 2009; Boumezbeur et al., 2010) and is accounted by V_{in} in the equations of brain pyruvate. In addition, V_{out} represents ^{13}C labeling dilution from the glycolysis, either by lactate release from brain parenchyma or by glucose utilization in alternative pathways.

Since scrambling of blood ^{13}C glucose and lactate enrichment may occur during peripheral metabolism and enrich carbons other than glucose C1 and C6 and lactate C3. These carbons are metabolized and lead to enrichment of pyruvate C2 that, by pyruvate carboxylation, contributes to direct enrichment of oxaloacetate C2. The following expression was defined but, in the absence of substantial enrichment of glucose C2 or C5 and lactate C2, it leads to simple dilution of oxaloacetate C2 while C3 is enriched in the glial compartment.

$$\frac{\mathrm{d}^{13}\mathrm{Pyr_2}}{\mathrm{dt}} = \mathrm{CMR_{glc}}\left(\frac{^{13}\mathrm{Glc_2}(t) + {}^{13}\mathrm{Glc_5}(t)}{\mathrm{Glc}(t)}\right) + V_{\mathrm{in}}\frac{^{13}\mathrm{Lac_2}(t)}{\mathrm{Lac}(t)} - \left(V_{\mathrm{out}} + V_{\mathrm{TCA}}^{\mathrm{n}} + V_{\mathrm{TCA}}^{\mathrm{g}} + V_{\mathrm{PC}}\right)\frac{^{13}\mathrm{Pyr_2}(t)}{\mathrm{Pyr}}.$$

Neuronal compartment

In the neuronal compartment, the concentration of ^{13}C-enriched TCA cycle intermediates is given by:

$$\frac{d^{13}OG_4^n}{dt} = V_{PDH}^n \frac{^{13}Pyr_3(t)}{Pyr} - \left(V_{PDH}^n + V_x^n\right)\frac{^{13}OG_4^n(t)}{OG^n} + V_x^n \frac{^{13}Glu_4^n(t)}{Glu^n}$$

$$\frac{d^{13}OG_3^n}{dt} = V_{PDH}^n \frac{^{13}OAA_2^n(t)}{OAA^n} - \left(V_{PDH}^n + V_x^n\right)\frac{^{13}OG_3^n(t)}{OG^n} + V_x^n \frac{^{13}Glu_3^n(t)}{Glu^n}$$

$$\frac{d^{13}OG_2^n}{dt} = V_{PDH}^n \frac{^{13}OAA_3^n(t)}{OAA^n} - \left(V_{PDH}^n + V_x^n\right)\frac{^{13}OG_2^n(t)}{OG^n} + V_x^n \frac{^{13}Glu_2^n(t)}{Glu^n}$$

$$\frac{d^{13}OAA_2^n}{dt} = \frac{V_{PDH}^n}{2}\left(\frac{^{13}OG_4^n(t) + {}^{13}OG_3^n(t)}{OG^n}\right) - \left(V_{PDH}^n + V_x^n\right)\frac{^{13}OAA_2^n(t)}{OAA^n} + V_x^n \frac{^{13}Asp_2^n(t)}{Asp^n}$$

$$\frac{d^{13}OAA_3^n}{dt} = \frac{V_{PDH}^n}{2}\left(\frac{^{13}OG_4^n(t) + {}^{13}OG_3^n(t)}{OG^n}\right) - \left(V_{PDH}^n + V_x^n\right)\frac{^{13}OAA_3^n(t)}{OAA^n} + V_x^n \frac{^{13}Asp_3^n(t)}{Asp^n}$$

In the neurons, ^{13}C glutamate, glutamine, and aspartate concentrations are given by the following expressions, where i can refer to any carbon position.

$$\frac{d^{13}Glu_i^n}{dt} = V_x^n \frac{^{13}OG_i^n(t)}{OG^n} - \left(V_{NT} + V_x^n\right)\frac{^{13}Glu_i^n(t)}{Glu^n} + V_{NT}\frac{^{13}Gln_i^n(t)}{Gln^n}$$

$$\frac{d^{13}Gln_i^n}{dt} = V_{NT}\left(\frac{^{13}Gln_i^g(t)}{Gln^g} - \frac{^{13}Gln_i^n(t)}{Gln^n}\right)$$

$$\frac{d^{13}Asp_i^n}{dt} = V_x^n\left(\frac{^{13}OAA_i^n(t)}{OAA^n} - \frac{^{13}Asp_i^n(t)}{Asp^n}\right)$$

Glial compartment

The glia comprises the additional fluxes through pyruvate carboxylase (V_{PC}) and glutamine synthesis (V_{GS}) (see Gruetter et al., 2001). In the glial compartment, a dilution factor was introduced at the level of acetyl-CoA (V_{dil}), accounting for possible ^{13}C label dilution by *in vivo* metabolism of acetate (Badar-Goffer et al., 1990; Cerdán et al., 1990; Deelchand et al., 2009), fatty acids (Ebert et al., 2003), or ketone bodies (Künnecke et al., 1993).

$$\frac{d^{13}AcCoA_2^g}{dt} = \left(V_g + V_{PC}\right)\frac{^{13}Pyr_3(t)}{Pyr} + V_{dil}\frac{^{13}Ac_2(t)}{Ac(t)} - \left(V_{dil} + V_g + V_{PC}\right)\frac{^{13}AcCoA_2^g(t)}{AcCoA^g}$$

Extra-cerebral acetate may contribute to brain metabolism and therefore ^{13}Ac represents blood-born ^{13}C acetate (**Figure 2C**). Transport of acetate into the brain was simulated as described by Deelchand et al. (2009) leading to enrichment of ^{13}Ac from plasma acetate.

Concentration of ^{13}C in carbons of glial TCA cycle intermediary metabolic pools is defined as follows:

$$\frac{d^{13}OG_4^g}{dt} = \left(V_g + V_{PC}\right)\frac{^{13}AcCoA_2^g(t)}{AcCoA^g} + V_x^g\frac{^{13}Glu_4^g(t)}{Glu^g} - \left(V_g + V_x^g + V_{PC}\right)\frac{^{13}OG_4^g(t)}{OG^g}$$

$$\frac{d^{13}OG_3^g}{dt} = \left(V_g + V_{PC}\right)\frac{^{13}OAA_2^g(t)}{OAA^g} + V_x^g\frac{^{13}Glu_3^g(t)}{Glu^g} - \left(V_g + V_x^g + V_{PC}\right)\frac{^{13}OG_3^g(t)}{OG^g}$$

$$\frac{d^{13}OG_2^g}{dt} = \left(V_g + V_{PC}\right)\frac{^{13}OAA_3^g(t)}{OAA^g} + V_x^g\frac{^{13}Glu_2^g(t)}{Glu^g} - \left(V_g + V_x^g + V_{PC}\right)\frac{^{13}OG_2^g(t)}{OG^g}$$

$$\frac{d^{13}OAA_2^g}{dt} = \frac{V_g}{2}\left(\frac{^{13}OG_4^g(t) + {}^{13}OG_3^g(t)}{OG^g}\right) + V_x^g\frac{^{13}Asp_2^g(t)}{Asp^g} + V_{PC}\frac{^{13}Pyr_2(t)}{Pyr} - \left(V_g + V_{PC} + V_x^g\right)\frac{^{13}OAA_2^g(t)}{OAA^g}$$

$$\frac{d^{13}OAA_3^g}{dt} = \frac{V_g}{2}\left(\frac{^{13}OG_4^g(t) + {}^{13}OG_3^g(t)}{OG^g}\right) + V_x^g\frac{^{13}Asp_3^g(t)}{Asp^g} + V_{PC}\frac{^{13}Pyr_3(t)}{Pyr} - \left(V_g + V_{PC} + V_x^g\right)\frac{^{13}OAA_3^g(t)}{OAA^g}$$

Concentration of ^{13}C in carbons of glial glutamate, glutamine, and aspartate is defined by the equations below, where i can refer to any carbon position.

$$\frac{d^{13}Glu_i^g}{dt} = \left(V_x^g + V_{PC}\right)\frac{^{13}OG_i^g(t)}{OG^g} - \left(V_{GS} + V_x^g\right)\frac{^{13}Glu_i^g(t)}{Glu^g} + V_{NT}\frac{^{13}Glu_i^n(t)}{Glu^n}$$

$$\frac{d^{13}Gln_i^g}{dt} = V_{GS}\frac{^{13}Glu_i^g(t)}{Glu^g} - \left(V_{NT} + V_{efflux}\right)\frac{^{13}Gln_i^g(t)}{Gln^g}$$

$$\frac{d^{13}Asp_i^g}{dt} = V_x^g\left(\frac{^{13}OAA_i^g(t)}{OAA^g} - \frac{^{13}Asp_i^g(t)}{Asp^g}\right)$$

REMOVING TCA CYCLE INTERMEDIATES FROM THE MODEL

Simplification of the mathematical model of cerebral metabolism was used to remove TCA cycle intermediates from mathematical expressions, as previously suggested by simulations (Uffmann and Gruetter, 2007).

For the sake of example, the combination of equations for neuronal glutamate C4 ($\frac{d^{13}Glu_4^n}{dt}$) and 2-oxoglutarate C4 ($\frac{d^{13}OG_4^n}{dt}$) can be used to eliminate terms with $\frac{^{13}OG_4^n(t)}{OG^n}$, leading to the following expression:

$$\frac{d^{13}Glu_4^n}{dt} + \frac{V_x^n}{V_{PDH}^n + V_x^n}\frac{d^{13}OG_4^n}{dt} = \frac{V_x^n V_{PDH}^n}{V_{PDH}^n + V_x^n}\frac{^{13}Pyr_3(t)}{Pyr} - \left(\frac{V_x^n V_{PDH}^n}{V_{PDH}^n + V_x^n} + V_{NT}\right)\frac{^{13}Glu_4^n(t)}{Glu^n} + V_{NT}\frac{^{13}Gln_4^n(t)}{Gln^n}.$$

Because the concentration of glutamate is much larger than that of the TCA cycle intermediates, the increase in concentration of glutamate enriched carbons is much larger at metabolic steady-state, i.e., $\frac{d^{13}Glu_4^n}{dt} >> \frac{d^{13}OG_4^n}{dt}$. Therefore, the expression can be approximated to

$$\frac{d^{13}Glu_4^n}{dt} = \frac{V_x^n V_{PDH}^n}{V_{PDH}^n + V_x^n}\frac{^{13}Pyr_3(t)}{Pyr} - \left(\frac{V_x^n V_{PDH}^n}{V_{PDH}^n + V_x^n} + V_{NT}\right) \times \frac{^{13}Glu_4^n(t)}{Glu^n} + V_{NT}\frac{^{13}Gln_4^n(t)}{Gln^n}.$$

Applying the same procedure to neuronal glutamate C3 (Glu_3^n), we obtain the following expression:

$$\frac{d^{13}Glu_3^n}{dt} = \frac{V_x^n V_{PDH}^n}{V_{PDH}^n + V_x^n}\frac{^{13}OAA_2^n(t)}{OAA^n} - \left(\frac{V_x^n V_{PDH}^n}{V_{PDH}^n + V_x^n} + V_{NT}\right) \times \frac{^{13}Glu_3^n(t)}{Glu^n} + V_{NT}\frac{^{13}Gln_3^n(t)}{Gln^n}.$$

From this expression, the term with oxaloacetate (OAA) can be removed by intermediary of the respective differential equation of aspartate, originating the expression:

$$\frac{d^{13}Glu_3^n}{dt} = \frac{V_{PDH}^n}{V_{PDH}^n + V_x^n}\left(\frac{d^{13}Asp_2^n}{dt} + V_x^n\frac{^{13}Asp_2^n(t)}{Asp^n}\right) - \left(\frac{V_x^n V_{PDH}^n}{V_{PDH}^n + V_x^n} + V_{NT}\right)\frac{^{13}Glu_3^n(t)}{Glu^n} + V_{NT}\frac{^{13}Gln_3^n(t)}{Gln^n}$$

With the same treatment for Glu_2^n originates the expression:

$$\frac{d^{13}Glu_2^n}{dt} = \frac{V_{PDH}^n}{V_{PDH}^n + V_x^n}\left(\frac{d^{13}Asp_3^n}{dt} + V_x^n\frac{^{13}Asp_3^n(t)}{Asp^n}\right) - \left(\frac{V_x^n V_{PDH}^n}{V_{PDH}^n + V_x^n} + V_{NT}\right)\frac{^{13}Glu_2^n(t)}{Glu^n} + V_{NT}\frac{^{13}Gln_2^n(t)}{Gln^n}$$

The same can be applied to equations of aspartate and we obtain the following expression where i can be any aliphatic carbon of aspartate.

$$\frac{d^{13}Asp_i^n}{dt} = \frac{V_{PDH}^n}{2\left(V_{PDH}^n + V_x^n\right)}\left(\frac{d^{13}Glu_4^n}{dt} + \frac{d^{13}Glu_3^n}{dt} + \left(V_{NT} + V_x^n\right)\frac{^{13}Glu_4^n(t) + ^{13}Glu_3^n(t)}{Glu^n} - V_{NT}\frac{^{13}Gln_4^n(t) + ^{13}Gln_3^n(t)}{Gln^n}\right) - \frac{V_x^n V_{PDH}^n}{V_{PDH}^n + V_x^n}\frac{^{13}Asp_i^n(t)}{Asp^n}$$

A similar approach in the glial compartment will originate the following equations for carbons of glutamate:

$$\frac{d^{13}Glu_4^g}{dt} = \frac{\left(V_x^g + V_{PC}\right)\left(V_g + V_{PC}\right)}{V_g + V_x^g + V_{PC}}\frac{^{13}AcCoA_2^g(t)}{AcCoA^g} + V_{NT}\frac{^{13}Glu_4^n(t)}{Glu^n} - \frac{V_{GS}\left(V_g + V_x^g + V_{PC}\right) + V_x^g V_g}{V_g + V_x^g + V_{PC}}\frac{^{13}Glu_4^g(t)}{Glu^g}$$

$$\frac{d^{13}Glu_3^g}{dt} = \frac{\left(V_x^g + V_{PC}\right)\left(V_g + V_{PC}\right)}{V_x^g\left(V_g + V_x^g + V_{PC}\right)}\frac{d^{13}Asp_2^g}{dt} + \frac{\left(V_x^g + V_{PC}\right)\left(V_g + V_{PC}\right)}{V_g + V_x^g + V_{PC}}\frac{^{13}Asp_2^g(t)}{Asp^g} - \frac{V_{GS}\left(V_g + V_x^g + V_{PC}\right) + V_x^g V_g}{V_g + V_x^g + V_{PC}}\frac{^{13}Glu_3^g(t)}{Glu^g} + V_{NT}\frac{^{13}Glu_3^n(t)}{Glu^n}$$

$$\frac{d^{13}Glu_2^g}{dt} = \frac{\left(V_x^g + V_{PC}\right)\left(V_g + V_{PC}\right)}{V_x^g\left(V_g + V_x^g + V_{PC}\right)}\frac{d^{13}Asp_3^g}{dt} + \frac{\left(V_x^g + V_{PC}\right)\left(V_g + V_{PC}\right)}{V_g + V_x^g + V_{PC}}\frac{^{13}Asp_3^g(t)}{Asp^g} - \frac{V_{GS}\left(V_g + V_x^g + V_{PC}\right) + V_x^g V_g}{V_g + V_x^g + V_{PC}}\frac{^{13}Glu_2^g(t)}{Glu^g} + V_{NT}\frac{^{13}Glu_2^n(t)}{Glu^n}$$

For the concentration of ^{13}C in carbons of glial aspartate, the following equation is obtained, where i can be either the position 2 or 3 in carbons of aspartate and pyruvate. Note that $^{13}Pyr_2$ and $^{13}Pyr_3$ will respectively label $^{13}OAA_2$ and $^{13}OAA_3$, and consequently $^{13}Asp_2$ and $^{13}Asp_3$.

$$\frac{d^{13}Asp_i^g}{dt} = \frac{V_x^g V_g}{2\left(V_g + V_{PC} + V_x^g\right)\left(V_x^g + V_{PC}\right)}\left(\frac{d^{13}Glu_4^g}{dt} + \frac{d^{13}Glu_3^g}{dt}\right) + \frac{V_x^g V_g}{2\left(V_g + V_{PC} + V_x^g\right)\left(V_x^g + V_{PC}\right)}\left[\left(V_{GS} + V_x^g\right)\left(\frac{^{13}Glu_4^g(t) + ^{13}Glu_3^g(t)}{Glu^g}\right) - V_{NT}\left(\frac{^{13}Glu_4^n(t) + ^{13}Glu_3^n(t)}{Glu^n}\right)\right] - \frac{V_x^g\left(V_g + V_{PC}\right)}{V_g + V_{PC} + V_x^g}\frac{^{13}Asp_i^g(t)}{Asp^g} + \frac{V_x^g V_{PC}}{V_g + V_{PC} + V_x^g}\frac{^{13}Pyr_i(t)}{Pyr}$$